Available online at www.sciencedirect.com
SCIENCE DIRECT®
Continental Shelf Research 24 (2004) 1001–1013
CONTINENTAL SHELF RESEARCH
www.elsevier.com/locate/csr

Assimilation of drifter and satellite data in a model of the Northeastern Gulf of Mexico

Shejun Fan[a], Lie-Yauw Oey[a,*], Peter Hamilton[b]

[a] *Program in Atmospheric and Oceanic Sciences, Princeton University, Princeton, NJ 08544-0710, USA*
[b] *Science Applications International Corporation, 615 Oberlin Road No. 100, Raleigh, NC 27605, USA*

Received 24 June 2003; received in revised form 22 January 2004; accepted 20 February 2004

Abstract

Drifter and satellite data are assimilated into a circulation model that hindcasts near-surface currents in the Northeastern Gulf of Mexico. Experiments without assimilation, and using assimilation of drifter, satellite sea-surface height (SSH) and sea-surface temperature (SST) data, in various combinations, were conducted. Currents derived from these experiments were used to compute drifter trajectories that were compared against observations. Surface geostropic current fields, calculated from satellite SSH, were also used to generate drifter paths. Assimilation that used a combination of drifter and satellite data reproduced the drifter trajectories with position errors $\approx$30–80 km over a 10-day period. Comparisons of the modeled currents with moored observations on the West Florida shelf show improvement when data assimilation is used, because of better simulation of deepwater processes (primarily the loop current).

Keywords: Data assimilation; Drifter; Satellite; Gulf of Mexico; Circulation model

1. Introduction

Predicting sea surface current field using ocean models is important for various applications, such as search and rescue operations and tracking mines, fish larvae and dispersal of pollutants. In the past decades, oceanographers, meteorologists, the US Navy and other agencies deployed a large number of ARGOS-tracked drifters in major ocean basins and some regional seas (Fratantoni, 2001; Poulain, 2001). The use of Lagrangian information to improve model predictability of sea surface current is a subject of active research (Mariano et al., 2002). Carter (1989) tested Kalman-filter technique to assimilate isopycnal RAFOS floats (in the Gulf Stream region) into a one-layer (reduced gravity) model in a periodic channel. Velocity vector and isopycnal depth were assimilated. Kamachi and O'Brien (1995) used simulated drifter trajectories from a control run as 'observations.' An adjoint method with variational

*Corresponding author. Tel.: +1-609-258-5971; fax: +1-609-258-2850.
E-mail addresses: lyo@splash.princeton.edu, lyo@princeton.edu (L.-Y. Oey).

0278-4343/$ - see front matter © 2004 Elsevier Ltd. All rights reserved.
doi:10.1016/j.csr.2004.02.013

formalism, employing a cost function based on the distance between the trajectories of the model drifters (from separate runs) and the 'observations', was developed. Ishikawa et al. (1996) conducted drifting buoy and altimetric data assimilation using nudging and optimal interpolation (OI) methods to determine the mean sea surface height as well as the temporal evolution of the surface circulation on synoptic scales. Ozgokmen et al. (2000, 2001) and Castellari et al. (2001) used Lagrangian particle models to assimilate drifter data. They solved a system of stochastic differential equations in which the Lagrangian velocity is made up of a deterministic part and a random component. Molcard et al. (2003) proposed an OI method to assimilate Lagrangian observation data into an Eulerian grid model. Most studies have considered idealized problems (i.e., simulated drifters and/or idealized domain) to test assimilation schemes. Casterllari et al. (2001) and Ozgokmen et al. (2001) used observed drifter data in realistic oceans, the former in the Adriatic Sea, a semi-enclosed sub-basin of the Mediterranean Sea, and the latter in the open tropical Pacific Ocean. Casterllari et al. (2001) showed observed-model drifter position errors of 35–65 km over 10 days. Ozgokmen et al. (2001) showed that these errors can be reduced (to <15 km over 7 days) if drifter data density (number of drifters over an area scaled by the mean diameter of the cluster) is large. Note that Casterllari et al. used surface drifters (so do we, see Section 2), which are sensitive to effects due to wind and wind wave. On the other hand, Ozgokmen et al.'s drifters are drogued at the 15-m depth level, making them relatively isolated from wind and wind wave.

In this study, a simple nudging scheme is used to assimilate observed drifters into a circulation model of the Northeastern Gulf of Mexico. The scheme is used in conjunction with an OI method that assimilates satellite sea-surface height (SSH) and sea-surface temperature (SST) data. The results are compared with a model experiment that has no assimilation and other experiments that use various combinations of SSH, SST and drifter data. The primary objective is to evaluate the extent that observed trajectories and circulation may be more accurately modeled when both satellite and drifter information are used. It is also demonstrated that data assimilation can effect the correct placement of Loop Current at the shelf edge; the Loop Current in turn (remotely) forces the currents on the West Florida shelf.

The paper is organized as follows: the drifter data are described in Section 2. In Section 3, we briefly review the model, as well as the satellite and drifter data assimilation schemes. The different experiments are described in Section 4, and results and analyses are presented in Section 5. Summary and conclusions follow in Section 6.

2. Drifter data

Drifter data were collected by the US Minerals Management Service (MMS) program: "Collection of Environmental Data for Oil Spill Risk Analysis Model Verification (CEDOMV)", which was part of the MMS Northeastern Gulf of Mexico Shelf Physical Oceanography Program (NEGOM, DiMarco et al., 2001). A total of 30 drifters, designed to drift at the surface within the upper 1 m and tracked by the ARGOS satellite system, were deployed from November 1997 to December 1999. For the present study, eight of the nine drifters deployed from 11 May 1998 to 10 July 1998 are used (negom20011 to negom20019). Negom20015 went ashore and is excluded from our analysis. Fig. 1 shows drifter trajectories. Note that the drifters are confined to shelf and slope regions where water depths <2500 m.

Positions of the drifters were smoothed using a Gaussian-filter scale of 24 h to eliminate tidal and inertial currents, and were sub-sampled at 3-h intervals. The method is given in Hamilton et al. (1999). Velocity components were then estimated from centered finite differences.

3. Methodology

3.1. Numerical model

The Princeton Ocean Model (Mellor, 2002) uses an orthogonal curvilinear grid system that covers the Gulf of Mexico, the Caribbean Sea and a portion of the Atlantic Ocean (Fig. 2; Oey and

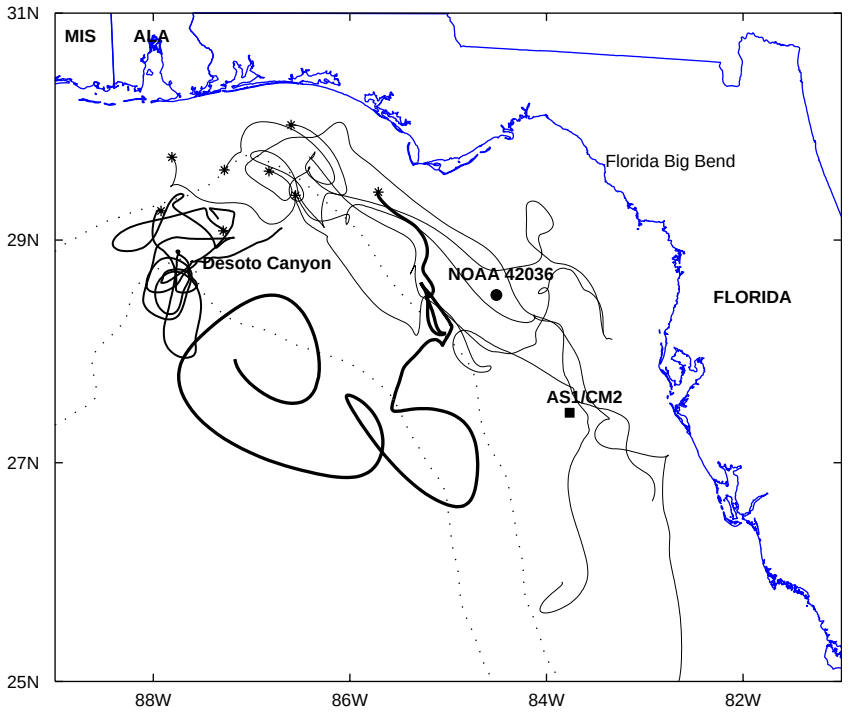

Fig. 1. Drifter trajectories in the northeastern Gulf of Mexico from 11 May 1998 to 10 July 1998. Initial drifter deployment locations are marked (*). Trajectories are grouped into three categories: (1) Shelf (thin solid curves), (2) Canyon (medium-solid curves), and (3) Lone Drifter (thick solid curve). The NOAA buoy 42036 and the ADCP site at the 50 m (AS1/CM2) isobath from the University of South Florida are also shown. The two dotted curves are 200 and 2000 m isobaths.

Lee, 2002). The approximate distribution of grid sizes in the Gulf is about 5 km in the northeastern Gulf, and 10 km near the Yucatan Channel. The model uses 25 sigma levels in the vertical, with higher resolution near the surface and the bottom. Table 1 shows the z-positions of the first model velocity point near the surface for various representative water depths. We see that the near-surface velocity points are within ± 1 m of the drifters' depth ($=-1$ m below the surface), and drifter-assimilation can be expected to be quite effective. Time-independent inflow and outflow that account for the large-scale transports (Svedrup + thermohaline) are specified across the open boundary at 55°W as a function of latitude as shown in Fig. 2. The three-dimensional velocity, temperature and salinity fields at the open boundary are calculated according to Oey and Chen (1992). For example, the temperature and salinity fields are advected using one-sided difference scheme when flows are eastward (that is, outflow), and are prescribed from the Generalized Digital Environmental Model (GDEM) monthly temperature and salinity climatology (Teague et al., 1990) when flows are westward. These open-boundary specifications also determine the baroclinic structure, which in the present case is largely geostrophic through the thermal-wind balance. The prescribed open boundaries are sufficiently removed from the Gulf of Mexico that there is a free dynamical interaction between the Caribbean Sea and the Gulf of Mexico through the Yucatan Channel (Oey, 1996). Surface forcing includes wind stress at 6-h intervals obtained from the European Center for Medium-Range Weather Forecast (ECMWF), and heat and salt fluxes based on monthly climatology. A recent POM study by Mellor and Blumberg (2004) shows that near-surface currents can depend on surface source of turbulence related to wind wave (i.e.

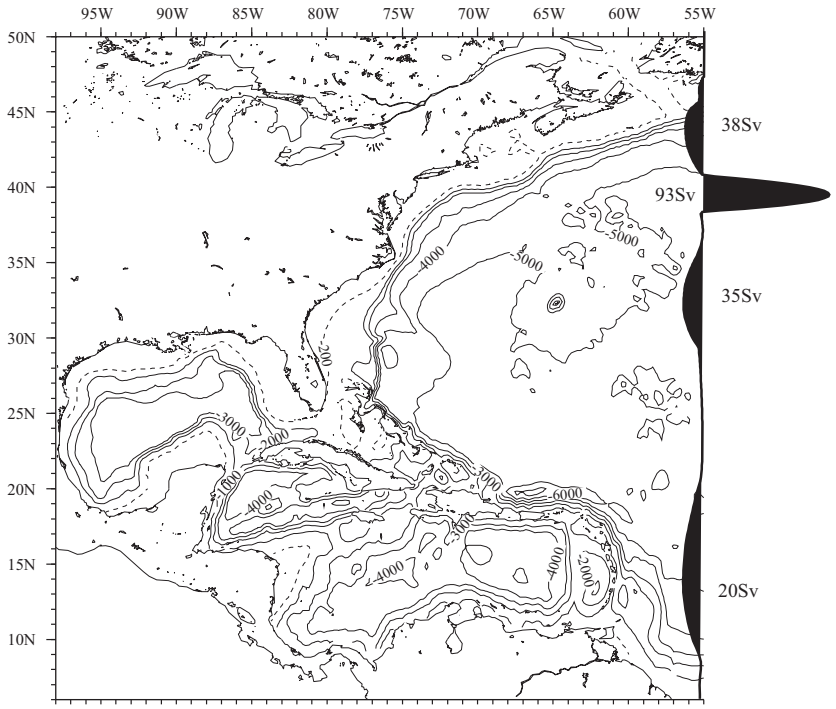

Fig. 2. Model domain. The model orthogonal curvilinear grids encompass the Gulf of Mexico, the Caribbean Sea, and a portion of the Atlantic Ocean. Time-independent inflow and outflow that account for the large-scale transports (Svedrup + thermohaline) are specified across the open boundary at 55°W as a function of latitude.

Table 1
The z-positions (in meters below mean sea-surface) of the first model velocity point near the surface for various representative water depths from 500 to 4000 m

	Water depths (m)							
	500	1000	1500	2000	2500	3000	3500	4000
Near-Surface (u,v) Z-Position (m)	−0.35	−0.70	−1.05	−1.40	−1.75	−2.10	−2.45	−2.80

the velocity profile is no longer logarithmic very near the surface; Craig and Banner, 1994). This new implementation is not used in the version of POM used here. For the satellite data assimilation experiments, satellite-derived sea surface temperature and altimeter data were used (Wang et al., 2003).

3.2. Assimilation scheme

3.2.1. Satellite data assimilation

The satellite SST and SSH were assimilated into the model following the methodology given in Mellor and Ezer (1991). First, the model is integrated without assimilation for 10 years. Correlations between (model) sea level anomaly ($\delta\eta$) and subsurface temperatures and salinities (T and S) were calculated from the model results, and are relatively high (>0.6) over a substantial portion of the gulf down to 500 m, but are reduced near the continental slope and rise. The maps of satellite SSH anomalies were created by merging TOPEX/Poseidon (T/P) and ERS-1 and -2 altimeter measurements (Ducet et al., 2000). Given the satellite Sea Surface Height Anomaly, $\delta\eta_{sa}$, the

model subsurface temperature anomaly δT is calculated from

$$\delta T(x,y,z,t) = F_T(x,y,z)\delta\eta_{sa}(x,y,t), \quad (1)$$

where the correlation factor is

$$F_T = \langle \delta T \delta\eta \rangle / \langle \delta\eta^2 \rangle, \quad (2a)$$

and the corresponding correlation coefficient is

$$C_T = \langle \delta T \delta\eta \rangle / (\langle \delta T^2 \rangle \langle \delta\eta^2 \rangle)^{1/2} \quad (2b)$$

After each assimilation time step Δt_A ($=1$ day), the model temperature T is replaced by assimilated temperature T_A, given by (see Mellor and Ezer, 1991, for details)

$$T_A = T + [2R_A C_T^2/(1 + 2R_A C_T^2 - C_T^2)] \times (T_o - T), \quad (3)$$

where R_A is the ratio of Δt_A to the de-correlation timescale Δt_E of the model eddy field (≈ 30 days), and T_o is the "observed" temperature inferred from satellite Sea Surface Height Anomaly. Thus, from (1)

$$T_o = \langle T \rangle + F_T \delta\eta_{sa}, \quad (4)$$

where $\langle T \rangle$ is taken here to be T_C, the climatological mean temperature (rather than the model mean). The effect of the assimilation is such that $T_A \approx T_o$ and $T_A \approx T$, in regions where the correlations are high and low, respectively. A similar assimilation of SST is also carried out using (3), with the same Δt_A, but with C_T and F_T replaced by the corresponding functions that use δ(SST) in place of $\delta\eta$ in (4). Weekly multichannel satellite SST maps were obtained from the Jet Propulsion Laboratory (JPL). The SSH assimilation is applied to regions where water depths are greater than 500 m.[1] However, the SST assimilation uses the entire region, including the shelves as well as deep waters. Sensitivity experiments indicate that the SSH and SST assimilations complement each other, with the deep portions of the Gulf being most affected by the former, while the latter has the most influence over the shelves.

[1] We have also tested SSH-assimilation over the entire region. The results are not sensitive.

3.2.2. Drifter data assimilation scheme

The velocity data, derived from drifting buoys, are assimilated into the model with a nudging method. A nudging term is introduced in the equation of motion as

$$\partial u/\partial t = (\text{physics}) - \lambda(u - u^o), \quad (5)$$

where "physics" includes Coriolis, pressure gradients, vertical divergence of shear stress, nonlinear advection, and other smaller terms such as the horizontal mixing. Ishikawa et al. (1996) proposed the following empirical equation for the nudging parameter λ:

$$\lambda = (1/t_a)\exp(-r^2/R_{nudge}^2) \times \exp(-(t - t^o)/t_d)\exp(z/z_d), \quad (6)$$

where r is the distance between the grid point in the model and the observation point (drifter position) and $(t-t^o)$ is the difference between the assimilation and observation time.[2] The assimilation timescale, t_a, determines the strength of the nudging factor, and the damping timescale, t_d, and lengthscale, R_{nudge}, are parameters of the nudging term. The $\exp(z/z_d)$ term, where $z_d = 10$ m, is used to restrict the effect of the assimilation to approximately the near-surface. (note that $z = 0$ at the mean sea-surface). It is found that using $t_a = 675$ s (the model's internal time step), $t_d = 1$ day, and $R_{nudge} = 0.4^\circ$ give satisfactory results. The method generates sources and sinks of momentum near the observation locations. Model dynamics then react to these 'forces' by changes, for example, in the corresponding pressure fields (through geostrophy), and information is imparted to neighboring (three-dimensional) grid points. This simple method was found to be robust and efficient.

Given $N(t)$ drifters active in the model region, at time t, λ may be calculated by local and weighted approaches, discussed below.

3.2.2.1. Local approach. If a drifter enters a cell centered on the model grid point (i,j) nearest the

[2] It is easy to show that nudging is a special case of the standard OI in which the gain matrix is analytically specified (as in here with λ) rather than derived by minimizing the square of the analysis error (Daley, 1991).

surface, at time t^o, then

$r_{i,j} = 0$, and from (6),

$$\lambda_{i,j} = (1/t_a)\exp(-(t - t^o_{i,j})/t_d), \quad (7)$$

where $r_{i,j}$, $\lambda_{i,j}$, and $t^o_{i,j}$, the time of the most recent drifter that enters the grid cell, are relative to the point (i,j).

Otherwise,

$$\lambda_{i,j} = 0 \quad (8)$$

3.2.2.2. Weighted approach. If there are N drifters, the algorithm is modified as

$$\frac{\partial u}{\partial t} = (\text{physics}) - \sum_{n=1}^{N} \lambda_n (u - u^o_n)/N, \quad (9)$$

$$\lambda_n = (1/t_a)\exp(-r^2_n/R^2_{nudge})\exp(-(t - t^o_n)/t_d. \quad (10)$$

Thus neighboring drifters influence the velocity at a particular grid cell where assimilation is effected.

3.3. Model drifters

Drifter positions were input into the model using the observations from 11 May 1998–10 July 1998. The simulated trajectories are calculated from the model Eulerian velocity field following Awaji et al. (1980). In order to increase the number of samples for error analysis, a re-sampling strategy is used. The 60-day model trajectories are divided into segments of n days. At the end of each segment, the model trajectories are reset to the observed drifter positions at that time. Each of the segments can, therefore, be considered as statistically independent, thereby increasing the number of trajectories available for the analysis. Previous studies (Casterllari et al., 2001; Ozgokmen et al., 2001) indicate that the predictability of drifter trajectories degrade considerably in 7–10 days. This study uses $n = 10$.

3.4. Error analysis

To quantify the performance of the assimilation scheme, the trajectory prediction error, $S(t)$, is defined as (Casterllari et al., 2001; Ozgokmen et al., 2001)

$$S(t) = \langle (r(t) - r_o(t))^2 \rangle^{1/2}, \quad (11)$$

where $r_o(t)$ and $r(t)$ are the observed and model drifter positions, respectively, computed using initial positions $r_o(0)$. The angle brackets denote ensemble averaging over all active drifters.

4. Model experiments

In order to compare the effectiveness of various assimilation schemes, seven experiments were conducted (Table 2). Experiment A has no assimilation, and is used as a base against which the assimilation studies can be compared. Experiment B adds satellite SSH and SST assimilations, and experiment C includes the satellite observations as well as the local drifter method, while experiment D uses only the local drifter assimilation. Similarly, experiment E has satellite SSH, SST and weighted drifter assimilation, and experiment F has only weighted drifter assimilation. Experiments B, C, D, E and F all start at the same time with the same initial conditions corresponding to April 20 1998 from experiment B. In this way, the effects of drifter velocity assimilation can be quantified by comparing the results of these experiments.

5. Results

5.1. Lagrangian predictability analysis

Lagrangian predictability is important for practical applications. Here the Lagrangian predict-

Table 2
Model experiments

Experiment no.	SSH and SST assimilation	Drifter assimilation
A	N = no	N
B	Y = yes	N
C	Y	Y (local)
D	N	Y (local)
E	Y	Y (weighted)
F	N	Y (weighted)

ability is quantified using Eq. (11), the root mean square error of the predicted differences with observations as a function of time and as the average of all drifters. Numerical trajectories, starting and ending at the times coinciding with the beginnings and endings of the observed drifter tracks, were calculated using model surface velocities. In order to increase the number of samples for error analysis, the 10-day re-sampling strategy was used as explained previously.

Fig. 3 shows the prediction errors for 10-day re-sampled drifters for all experiments. Assimilation using only satellite data (experiment B) does not improve Lagrangian prediction; the errors for experiment A and B are approximately the same. The errors decrease when drifter observations are also included (experiments C–F). The error is least in experiment E when both satellite data and weighted drifters are assimilated.

It is instructive to study the behavior of the drifters in three groups (Fig. 1). The shelf group includes five drifters that remained generally on the shelf during the observation period, the canyon group consists of two drifters that went into the DeSoto Canyon, and lastly the lone drifter that moved from the shelf southward into deep-water region.

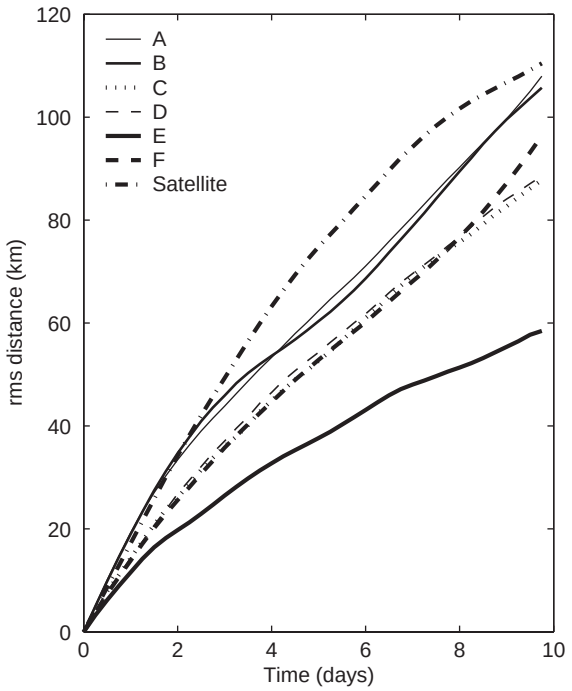

Fig. 3. The prediction errors for 10-day re-sampled drifters for all experiments.

5.1.1. Shelf group

Two examples of observed and modeled drifter trajectories for the shelf group are shown in Fig. 4, where solid lines indicate the observed trajectories. Thin, medium and heavy dotted lines are 10-day

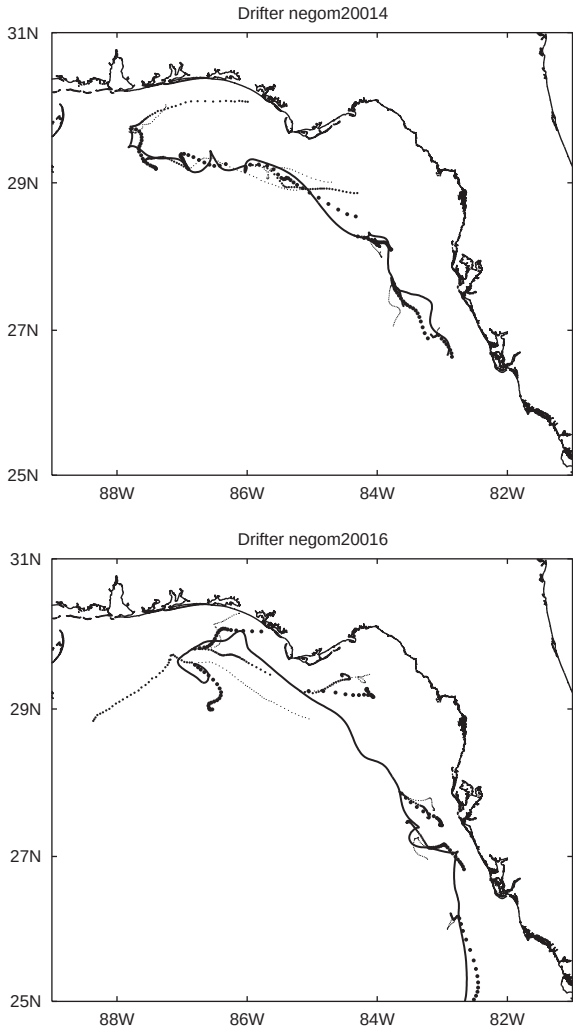

Fig. 4. Observed (Solid Lines) and modeled trajectories for drifter #0014 (upper panel) and #0016 (lower panel) of shelf group. Thin, medium and heavy dotted lines are 10-day re-sample modeled trajectories of experiments A, B and E, respectively. Time interval between two consecutive dots is six hours.

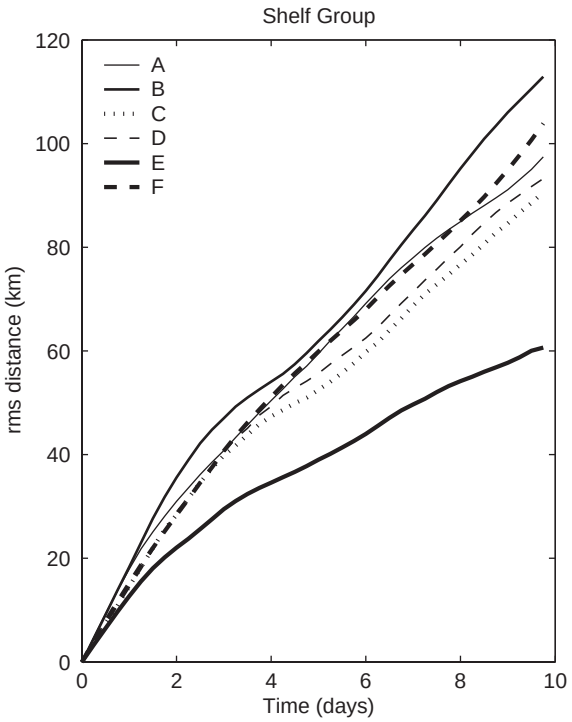

Fig. 5. The prediction errors for 10-day re-sampled drifters of the shelf group.

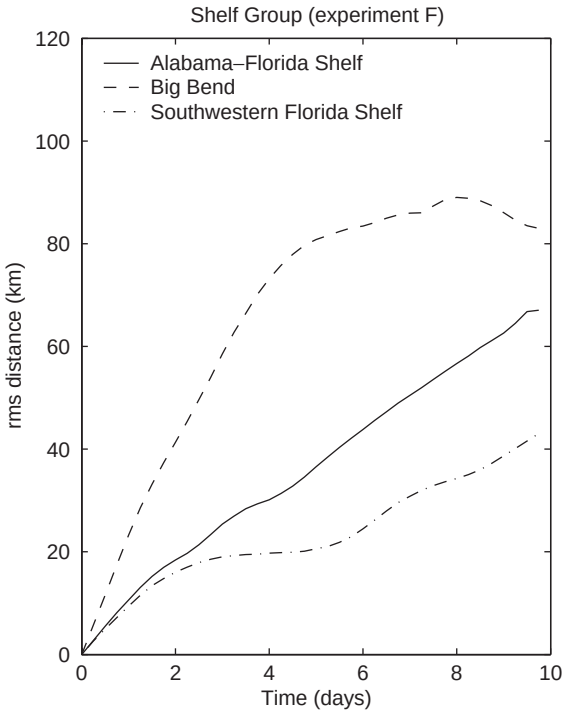

Fig. 6. The prediction errors for 10-day re-sampled drifters of the shelf group for experiment F. The prediction errors are further divided into the three subgroups as shown.

re-sampled trajectories for experiments A, B and E, respectively. Without drifter assimilation, the model trajectories tend to drift away from the observed trajectories on the northern shelf (the Alabama-Florida shelf) and underestimate the velocity or the total displacement of the drifters on southwestern Florida shelf. Inclusion of satellite data assimilation (experiment B) does not seem to improve the simulated currents, but inclusion of the drifters improves the model currents. The trajectories for experiment E (with SSH, SST and weighted drifter assimilation) generally follow the observed trajectories, except for the Florida Big Bend where there were no drifter observations (Fig. 1).

In Fig. 5, the prediction errors are shown for all the seven experiments. Satellite assimilation (B) actually increases the error when compared with the experiment without assimilation (A). Thus, the model without assimilation displays some skill on the shelf. Inclusion of the drifters reduces the errors (experiments C, D and F), however experiment E, with a combination of satellite and weighted drifter assimilation, gives the smallest error. Fig. 6 divides the prediction errors of experiment E into three regions. The errors are largest on the northeast (Big Bend) shelf. The errors on the southwestern Florida shelf, are the least, probably because of the relative simple flows in this region.

5.1.2. Canyon group

Two drifters went into DeSoto Canyon during the observation period (5/11/1998 to 7/10/1998). The observed and modeled drifter trajectories for these two drifters are shown in Fig. 7 where again solid lines indicate the observed trajectories. Thin, medium and heavy dotted lines are modeled trajectories for experiments A, B and E, respectively. The observed trajectories indicate a small cyclone in the canyon. The drifter assimilation experiments (C, D, E and F) could simulate this small current feature, while experiments without drifter assimilation could not. In particular, the

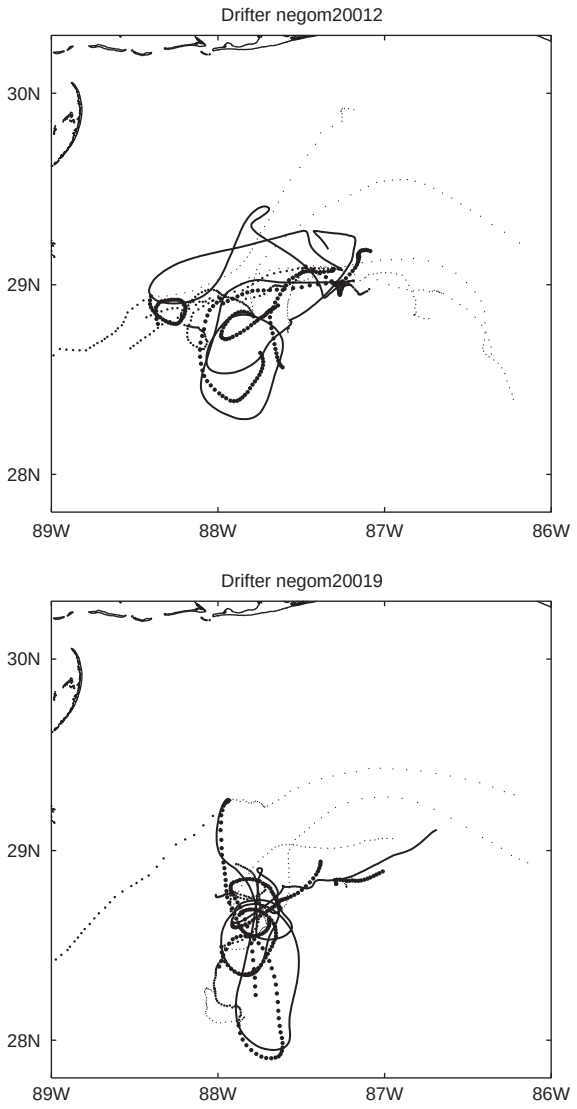

Fig. 7. Observed (Solid lines) and simulated trajectories for drifter #0012 (upper panel) and #0019 (lower panel) of the canyon group. Thin, medium and heavy dotted lines are 10-day re-sample modeled trajectories of experiments A, B and E, respectively. Time interval between two consecutive dots is six hours.

weighted drifter assimilations (E and F) yield the least prediction errors (Fig. 8).

5.1.3. Lone drifter

The lone drifter moved from shelf to deep water during the observation period (5/11/1998 to 7/10/1998). The observed and simulated trajectories are

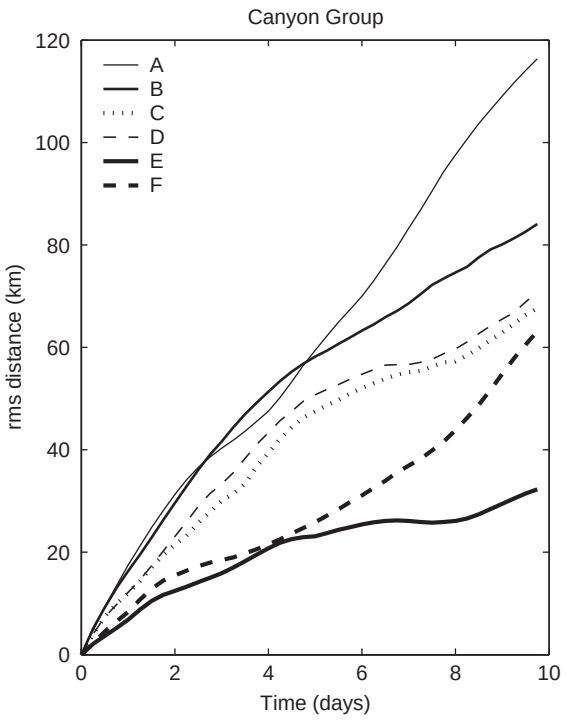

Fig. 8. The prediction errors for 10-day re-sampled drifters in the canyon group for all experiments.

shown in Fig. 9, where in this case, the thin, medium and heavy dotted lines are modeled trajectories for experiments A, B and E, respectively. Similar to the shelf group, the predictability of all experiments is poor when the drifter was on the northeastern shelf. However, as the drifter moved into deep water, the predictability of experiment E improves and the modeled trajectories follow an anti-cyclonic path similar to that observed. Over deeper water, the prediction in this case appears to benefit from the assimilation of satellite data. The experiments without drifter assimilation tend to underestimate the velocity or the total displacement of the drifter, and during the last 10 days, modeled trajectories for experiments A and B stay near their initial locations and failed to follow the observed anti-cyclonic path. The prediction errors in this case (not shown) indicate similar improvements when drifters are assimilated, especially for the last 10 days where the eddy feature of the circulation is better simulated.

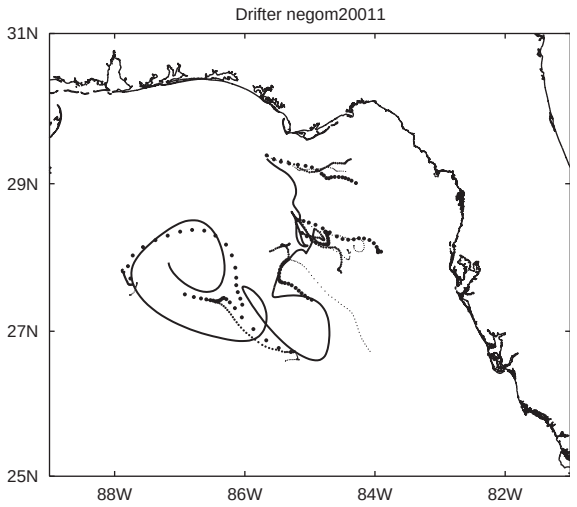

Fig. 9. Observed (Solid Lines) and simulated trajectories for drifter #0011 of the lone drifter. Thin, medium and heavy dotted lines are 10-day re-sample modeled trajectories of experiments A, B and E, respectively. Time interval between two consecutive dots is six hours.

Satellite SSH anomaly is added to the ten-year model mean SSH in order to calculate surface geostrophic currents. Fig. 10 compares the circulation obtained from 5-day averaged (from 7/6/1998 to 7/10/1998) geostrophic current field with those from experiments A, B and E. Of interest is the occurrence of a small anticyclonic eddy in experiment E at the location where the "lone drifter" was assimilated. This eddy is not apparent in A and B and is barely discernible in the satellite-derived geostrophic current field. The Lagrangian prediction errors are compared (Fig. 3), for all experiments, with those calculated from simulated drifter tracks that are derived from the surface geostrophic current field. The geostrophic currents can yield poor drifter prediction because of uncertainties in the mean SSH field (and satellite sampling errors). Fig. 10 also shows that assimilation of even a single drifter can yield a useful small-scale eddy field that was not detected by the satellite. Note also that while drifter assimilation is effective only in the near-surface 10 m of water ($z_d = 10$ m in Eq. (6)), the information is transmitted deeper (Fig. 10 is for $z = -27$ m) through modifications to the model's dynamics (e.g. pressure field).

5.2. Comparison with current measurement on the Florida shelf

Weisberg and He (2003) documented an interesting current event in the summer of 1998 at station AS1/CM2 (Fig. 1). Shelf flows were southward, fairly intense (~ 0.1 m/s) and uncorrelated with the wind. The authors attributed these currents to the close proximity of the Loop Current to the southern shelf and slope of the west Florida shelf. By experimenting with various specifications of the southern open boundary conditions of a west Florida shelf regional model they showed that the shelf current was remotely forced. Their hypothesis can be tested using the more general, Gulf-wide simulation results discussed above. Fig. 11 compares the observed current (lowest panel) with those obtained from experiments A, B and E. The top panel shows the wind stress and it is evident that there is little correlation between the wind and currents. Experiment A gives weak currents with a northward mean (over $5/11 \sim 7/10/98$ period) opposite to that observed. However, experiments B and E give more intense southward currents similar to those observed. In Fig. 10, it is seen from the model results that, in the Florida Straits, the Loop Current intrudes north over the Florida shelf. Strong currents extend inshore of the 200 m isobath.[3] On the other hand, the Loop Current, in experiment A, is near the Cuban side of the Straits and the strong shelf currents, widespread in experiments B and E, are restricted to the shelfbreak. Thus, it is clear that the broader southward shelf currents in experiment B and E are remotely forced by the Loop Current.

6. Conclusions

Assimilation of drifter and satellite data in a circulation model of the Northeastern Gulf of Mexico was explored by studying the Lagrangian predictability of drifter trajectories and surface current velocity field. Modeled drifter trajectories

[3] This holds even when SST is *not* assimilated over the shelves.

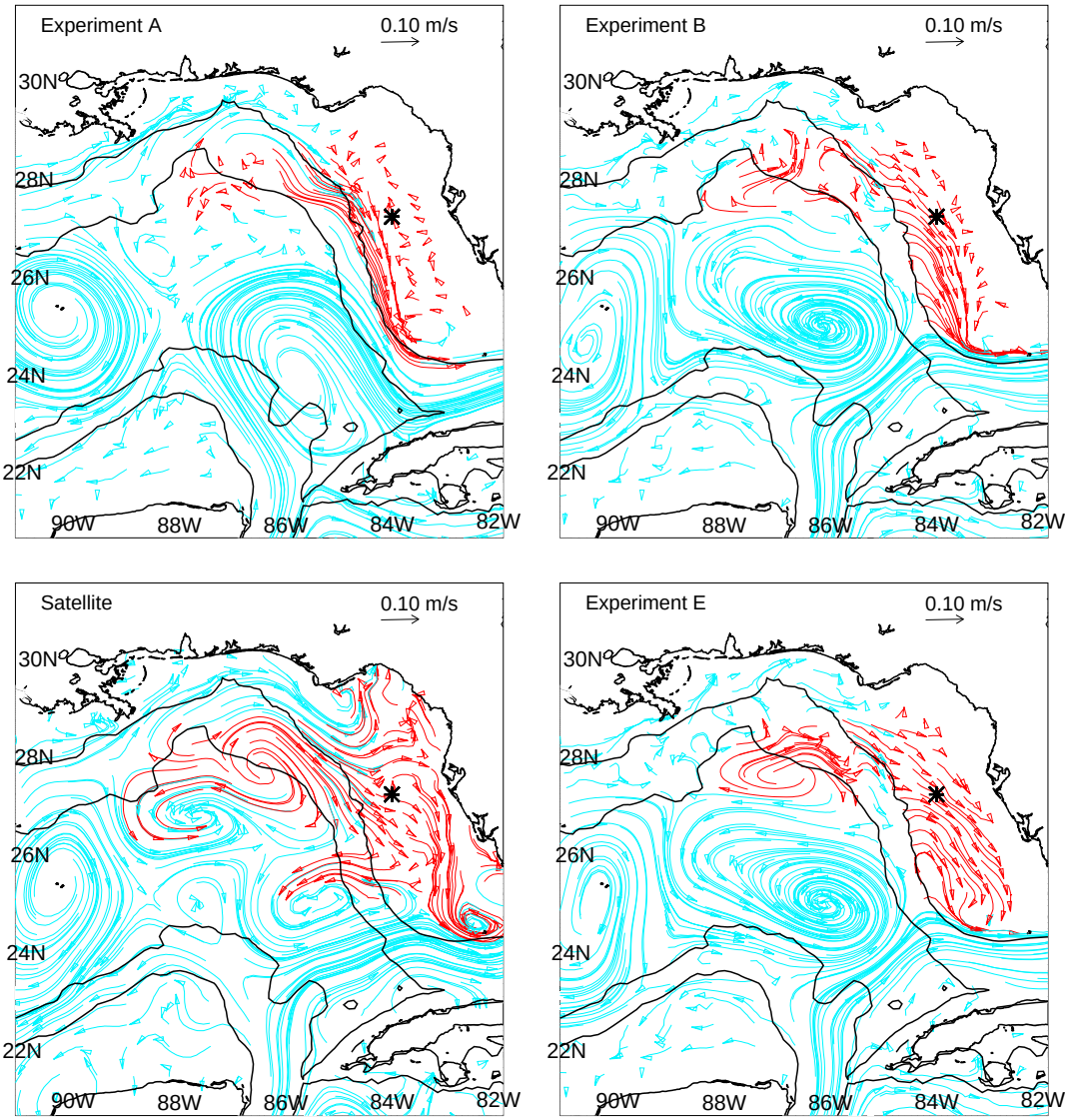

Fig. 10. Five-day averaged surface velocity ($z=-27$ m; plotted as Eulerian trajectories) from 6 July 1998 to 10 July 1998 for experiments A, B, satellite SSH derived geostrophic velocity, and experiment F. The asterisk denotes ADCP site AS1/CM2. The two solid line are 200 and 2000 m isobaths. Dark (red) curves (trajectories) emphasize west Florida shelf currents and lone-drifter eddy (experiment E or F) as discussed in text.

were compared for different experiments as well as with drifter observations. The model experiments included no assimilation (A), satellite SSH and SST assimilation (B), and other permutations of SSH, SST and drifter assimilations (C, D, E and F).

Numerical trajectories, which start and end at the times coincident with the beginnings and endings of the observed drifter tracks, were calculated using model surface velocities. The model prediction errors were then calculated as differences between the observed and modeled trajectories over consecutive 10-day periods. Comparison of prediction errors shows that assimilation, using satellite SSH, SST and drifter data, yields the least error. Drifter position errors range from 30–80 km with a mean of about 60 km

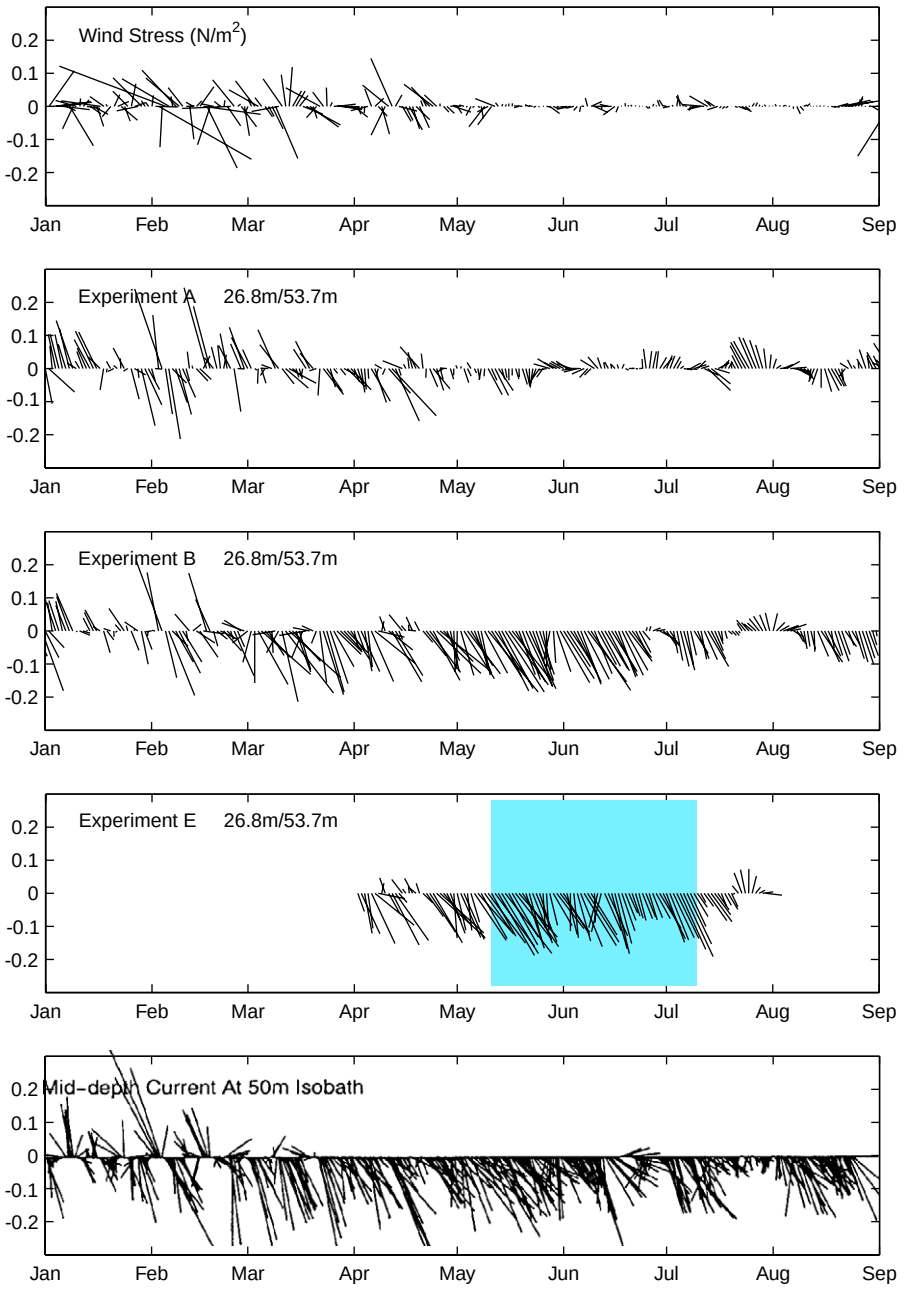

Fig. 11. Time series of winds, AS1/CM2 (on west Florida shelf, see Fig. 1 for location) mid-depth currents for experiment A, B, and E, and observed (bottom panel; Weisberg and He, 2003). The shaded area for experiment E is the time period with drifter assimilation.

over 10-day periods, which are comparable to errors obtained by Castellari et al. (2001). In particular, drifter assimilation can yield small-scale (diameter $\sim$100 km) eddies that are generally not resolved by satellite data. On the west Florida shelf, data assimilation over the deep ocean region can better simulate remote forcing that improves prediction of the shelf currents.

The drifter assimilation scheme (nudging) used is simple, yet highly efficient. Work is in progress to implement a multivariate optimal interpolation assimilation scheme. Future work should also explore the sensitivity of near-surface currents and drifter trajectories to assumptions on surface turbulence input by wind wave.

Acknowledgements

Constructive comments from two anonymous reviewers improved the manuscript. This study is supported by the Minerals Management Service under contracts #1435-01-00-CT-31076. Computing was conducted at GFDL/NOAA.

References

Awaji, T., Imasato, N., Kunishi, H., 1980. Tidal exchange through a strait: a numerical experiment using a simple model basin. Journal of Physical Oceanography 10, 1499–1508.

Carter, E.F., 1989. Assimilation of Lagrangian data into a numerical model. Dynamics of Atmospheres and Oceans 13, 335–348.

Castellari, S., Griffa, A., Ozgokmen, T.M., Poulain, P.M., 2001. Prediction of particle trajectories in the Adriatic sea using Lagrangian data assimilation. Journal of Marine Systems 29, 33–50.

Craig, P.D., Banner, M.L., 1994. Modeling wave-enhanced turbulence in the ocean surface layer. Journal of Physical Oceanography 24, 2546–2559.

Daley, R., 1991. Atmospheric Data Analysis. Cambridge University Press, New York, 457pp.

DiMarco, S.F., Howard, M.K., Jochens, A.E., 2001. Deep-water Gulf of Mexico historical Physical Oceanography and data inventory. Department of Oceanography, Texas A&M University, Technical Report 01-01-D, 196pp.

Ducet, N., Tron, P.Y. Le, Reverdin, G., 2000. Global high-resolution mapping of ocean circulation from TOPEX/Poseidon and ERS-1 and −2. Journal of Geophysics Research 105, 19477–19498.

Fratantoni, D.M., 2001. North Atlantic surface circulation during the 1990's observed with satellite-tracked drifters. Journal of Physical Oceanography 106, 22067–22093.

Hamilton, P., Fargion, G.S., Biggs, D.C., 1999. Loop Current eddy paths in the western Gulf of Mexico. Journal of Physical Oceanography 29, 1180–1207.

Ishikawa, Y.I., Awaji, T., Akimoto, K., 1996. Successive correction of the mean sea surface height by the simultaneous assimilation of drifting buoy and altimetric data. Journal of Physical Oceanography 26, 2381–2397.

Kamachi, M., O'Brien, J.J., 1995. Continuous data assimilation of drifting buoy trajectory into an equatorial Pacific Ocean Model. Journal of Marine Systems 6, 159–178.

Mariano, A.J., Griffa, A., Ozgokmen, T.M., Zambianchi, E., 2002. Lagrangian analysis and predictability of coastal and ocean dynamics 2000. Journal of Atmospheric and Oceanic Technology 19, 1114–1126.

Mellor, G.L., 2002. Users guide for a three-dimensional, primitive equation, numerical ocean model (July 2002 version). Program in Atmospheric and Oceanic Sciences, Princeton University, 42pp.

Mellor, G.L., Blumberg, A., 2004. Wave breaking and ocean surface layer thermal response. Journal of Physical Oceanography 34, 693–698.

Mellor, G.L., Ezer, T., 1991. A Gulf Stream model and an altimetry assimilation scheme. Journal of Geophysics Research 96, 8779–8795.

Molcard, A., Piterbarg, L.I., Griffa, A., Ozgokmen, T.M., Mariano, A.J., 2003. Assimilation of drifter observations for the reconstruction of the Eulerian circulation field. Journal of Geophysics Research 108 (C3), 3056, doi:10.1029/2001JC001240.

Oey, L.-Y., 1996. Simulation of mesoscale variability in the Gulf of Mexico. Journal of Physical Oceanography 26, 145–175.

Oey, L.-Y., Chen, P., 1992. A model simulation of circulation in the northeast Atlantic shelves and seas. Journal of Geophysics Research 97, 20087–20115.

Oey, L.-Y., Lee, H.C., 2002. Deep eddy energy and topographic Rossby waves in the Gulf of Mexico. Journal of Physical Oceanography 32, 3499–3527.

Ozgokmen, T.M., Griffa, A., Piterbarg, L.I., Mariano, A.J., 2000. On the predictability of the Lagrangian trajectories in the ocean. Journal of Atmospheric and Oceanic Technology 17/3, 366–383.

Ozgokmen, T.M., Piterbarg, L.I., Mariano A, J., Ryan, E.H., 2001. Predictability of drifter trajectories in the tropical Pacific Ocean. Journal of Physical Oceanography 31, 2691–2720.

Poulain, P.M., 2001. Adriatic Sea surface circulation as derived from drifter data between 1990 and 1999. Journal of Marine Systems 29, 3–32.

Teague, W.J., Carron, M.J., Hogan, P.J., 1990. A comparison between the Generalized Digital Environmental Model and Levitus climatologies. Journal of Geophysics Research 95, 7167–7183.

Wang, D.-P., Oey, L.-Y., Ezer, T., Hamilton, P., 2003. The near-surface currents in DeSoto Canyon (1997–1999): Observations, satellite data, and comparison with model simulations. Journal of Physics Oceanography 33, 313–326.

Weisberg, R.H., He, R., 2003. Local and deep-ocean forcing contributions to anomalous water properties on the West Florida shelf. Journal of Geophysics Research 108 (C6), 3184, doi:10.1029/2002JC001407.